Higher-Order Compact Scheme for the Incompressible Navier-Stokes Equations in Spherical Geometry

T. V. S. Sekhar[1,*], B. Hema Sundar Raju[1] and Y. V. S. S. Sanyasiraju[2]

[1] *Department of Mathematics, Pondicherry Engineering College, Puducherry-605 014, India.*
[2] *Department of Mathematics, Indian Institute of Technology Madras, Chennai-600 036, India.*

Abstract. A higher-order compact scheme on the nine point 2-D stencil is developed for the steady stream-function vorticity form of the incompressible Navier-Stokes (N-S) equations in spherical polar coordinates, which was used earlier only for the cartesian and cylindrical geometries. The steady, incompressible, viscous and axially symmetric flow past a sphere is used as a model problem. The non-linearity in the N-S equations is handled in a comprehensive manner avoiding complications in calculations. The scheme is combined with the multigrid method to enhance the convergence rate. The solutions are obtained over a non-uniform grid generated using the transformation $r = e^{\xi}$ while maintaining a uniform grid in the computational plane. The superiority of the higher order compact scheme is clearly illustrated in comparison with upwind scheme and defect correction technique at high Reynolds numbers by taking a large domain. This is a pioneering effort, because for the first time, the fourth order accurate solutions for the problem of viscous flow past a sphere are presented here. The drag coefficient and surface pressures are calculated and compared with available experimental and theoretical results. It is observed that these values simulated over coarser grids using the present scheme are more accurate when compared to other conventional schemes. It has also been observed that the flow separation initially occurred at $Re = 21$.

*Corresponding author. *Email addresses:* `sekhartvs@yahoo.co.in` (T. V. S. Sekhar), `rajubhs@rediffmail.com` (B. H. S. Raju), `sryedida@iitm.ac.in` (Y. V. S. S. Sanyasiraju)

1 Introduction

The complexity involved in solving N-S equations by numerical approximations differs for various geometries such as cartesian, cylindrical and spherical polar coordinates, especially while handling non-linearity of the N-S equations. The present paper is concerned with solving the steady two-dimensional Navier-Stokes equations in spherical polar coordinates using higher order compact scheme (HOCS) on the nine point 2-D stencil as shown in Fig. 1.
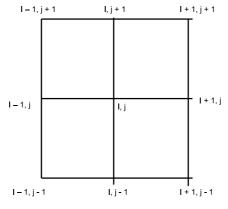

Figure 1: Nine point 2-D stencil.

The study of steady incompressible N-S equations using finite difference methods vary considerably in terms of accuracy and efficiency. The central difference approximations to all the derivatives of the N-S equations yields second order accuracy but the resulting solutions may exhibit non-physical oscillations. The combination of central differences to second order derivatives and first order upwind differences to nonlinear terms (here after denoted as CDS-UPS) as described by Ghia et al. [1], Juncu and Mihail [2] and Sekhar et al. [3] yields a stable scheme but is of first order accurate and the resulting solutions exhibit the effects of artificial viscosity. Also, at high *Re*, approximation of convective terms using CDS-UPS scheme may not capture the flow phenomena accurately due to the dominance of inertial forces. To capture the flow phenomena, at least second order accuracy is required. The second order upwind differences to nonlinear terms are no better than the first-order ones for large values of *Re* and also require ghost points. The second order accuracy can be achieved by employing defect correction technique (DC) for CDS-UPS scheme [1, 2]. The traditional higher order finite difference methods [4] contains ghost points and requires special treatment near the boundaries. If the domain is large, the above first and second order accurate methods may not converge with coarser grids and grid independence can be achieved only with very high finer grids which consumes more CPU time and memory [3]. An exception has been found in the high order finite difference schemes of compact type, which are computationally stable, efficient and yield highly accurate numerical solutions [5, 6]. Jiten et al. [7] developed

fully HOCS for steady state natural convection in cartesian coordinate system. Spotz and Carey [8] and Erturk and Gokcol [9] developed fourth order compact formulations for steady 2-D incompressible N-S equations in cartesian form. HOCS are less applied to flow problems in curvilinear coordinate systems like cylindrical and spherical polar coordinates. Iyengar and Manohar [10], Jain [11] and Lai [12] developed compact fourth order schemes to linear Poisson or quasi-linear Poisson equations in polar coordinates. Sanyasiraju and Manjula [13, 14] developed higher order *semi-compact* scheme to incompressible N-S equations in cylindrical coordinates in which compactness is relaxed for a few terms. Recently, Jiten and Rajendra [15] and Rajendra and Jiten [16] developed a transformation free HOCS for incompressible viscous flow past an impulsively started circular cylinder and for non-uniform polar grids respectively.

To the best of our knowledge, no work has been reported until now on HOCS to N-S equations in spherical polar coordinate system. In this work, a fourth order compact scheme is developed for steady, incompressible N-S equations in spherical polar coordinates. The steady, incompressible, viscous and axially symmetric flow past a sphere is used as a model problem. The multigrid method is combined with HOCS to enhance the convergence rate.

2   Basic equations

The flow of steady incompressible viscous flow past a sphere with uniform free-stream velocity U_∞ (from left to right) is considered for this study. The governing equations are equation of continuity:

$$\nabla \cdot q = 0, \tag{2.1}$$

momentum equation:

$$(q \cdot \nabla)q = -\nabla p + \frac{2}{Re}\nabla^2 q. \tag{2.2}$$

Taking curl on both sides of Eq. (2.2), we obtain

$$\nabla \times q \times \omega = \frac{2}{Re}(\nabla \times \nabla \times \omega), \tag{2.3}$$

where

$$\omega = \nabla \times q \tag{2.4}$$

is the vorticity and *Re* is the Reynolds number defined as $Re = 2U_\infty a/\nu$, where a is radius of the sphere and ν is kinematic coefficient of viscosity. The non-dimensional radial velocity (q_r) and transverse velocity (q_θ) components (which are obtained by dividing the corresponding dimensional components by the stream velocity U_∞) are chosen in such a way that the equation of continuity (2.1) is satisfied in spherical polar coordinates. They are

$$q_r = \frac{1}{r^2 \sin\theta}\frac{\partial \psi}{\partial \theta}, \qquad q_\theta = \frac{-1}{r\sin\theta}\frac{\partial \psi}{\partial r}. \tag{2.5}$$

Expanding (2.3) and (2.4), using (2.5) with spherical polar coordinates (r,θ,ϕ) (axis-symmetric), we get the Navier-Stokes equations in vorticity-stream function form as

$$\frac{\partial^2 \psi}{\partial r^2} + \frac{1}{r^2}\frac{\partial^2 \psi}{\partial \theta^2} - \frac{\cot\theta}{r^2}\frac{\partial \psi}{\partial \theta} = -r\omega\sin\theta,$$

$$\frac{\partial^2 \omega}{\partial r^2} + \frac{2}{r}\frac{\partial \omega}{\partial r} + \frac{1}{r^2}\frac{\partial^2 \omega}{\partial \theta^2} + \frac{\cot\theta}{r^2}\frac{\partial \omega}{\partial \theta} - \frac{\omega}{r^2\sin^2\theta} = \frac{Re}{2}\Big(q_r\frac{\partial \omega}{\partial r} + \omega\frac{\partial q_r}{\partial r} + \frac{q_r\omega}{r} + \frac{q_\theta}{r}\frac{\partial \omega}{\partial \theta} + \frac{\omega}{r}\frac{\partial q_\theta}{\partial \theta}\Big).$$

Because, the stream function and vorticity are expected to vary most rapidly near the surface of the sphere, we substitute $r = e^{\xi}$ so that the above two equations become in (ξ,θ) coordinates [23] as follows

$$\frac{\partial^2 \psi}{\partial \xi^2} - \frac{\partial \psi}{\partial \xi} + \sin\theta\frac{\partial}{\partial \theta}\Big(\frac{1}{\sin\theta}\frac{\partial \psi}{\partial \theta}\Big) + \sin\theta e^{3\xi}\omega = 0, \tag{2.6a}$$

$$\frac{\partial^2 \omega}{\partial \xi^2} + \frac{\partial \omega}{\partial \xi} + \cot\theta\frac{\partial \omega}{\partial \theta} + \frac{\partial^2 \omega}{\partial \theta^2} - \frac{\omega}{\sin^2\theta} = \frac{Re}{2}e^{\xi}\Big(q_r\frac{\partial \omega}{\partial \xi} + q_\theta\frac{\partial \omega}{\partial \theta} - q_r\omega - q_\theta\omega\cot\theta\Big), \tag{2.6b}$$

where ψ and ω are dimensionless stream function and vorticity respectively and

$$q_r = \frac{e^{-2\xi}}{\sin\theta}\frac{\partial \psi}{\partial \theta}, \qquad q_\theta = -\frac{e^{-2\xi}}{\sin\theta}\frac{\partial \psi}{\partial \xi}. \tag{2.7}$$

The boundary conditions to be satisfied are

$$\text{On the surface of the sphere } (\xi=0): \quad \psi = \frac{\partial \psi}{\partial \xi} = 0, \quad \omega = -\frac{1}{\sin\theta}\frac{\partial^2 \psi}{\partial \xi^2}.$$

$$\text{At large distances from the sphere } (\xi\to\infty): \quad \psi \sim \frac{1}{2}e^{2\xi}\sin^2\theta, \quad \omega\to 0.$$

$$\text{Along the axis of symmetry } (\theta=0 \text{ and } \theta=\pi): \quad \psi = 0, \quad \omega = 0.$$

3 Fourth order compact scheme with multigrid method

The standard fourth order central difference operators for the first and second order partial derivatives are given by the following equations

$$\frac{\partial \phi}{\partial \xi} = \delta_\xi\phi - \frac{h^2}{6}\frac{\partial^3 \phi}{\partial \xi^3} + \mathcal{O}(h^4), \qquad \frac{\partial^2 \phi}{\partial \xi^2} = \delta_\xi^2\phi - \frac{h^2}{12}\frac{\partial^4 \phi}{\partial \xi^4} + \mathcal{O}(h^4), \tag{3.1a}$$

$$\frac{\partial \phi}{\partial \theta} = \delta_\theta\phi - \frac{k^2}{6}\frac{\partial^3 \phi}{\partial \theta^3} + \mathcal{O}(k^4), \qquad \frac{\partial^2 \phi}{\partial \theta^2} = \delta_\theta^2\phi - \frac{k^2}{12}\frac{\partial^4 \phi}{\partial \theta^4} + \mathcal{O}(k^4), \tag{3.1b}$$

where $\delta_\xi\phi$, $\delta_\xi^2\phi$, $\delta_\theta\phi$ and $\delta_\theta^2\phi$ are the standard second order central differences given by

$$\delta_\xi\phi_{i,j} = \frac{\phi_{i+1,j} - \phi_{i-1,j}}{2h}, \qquad \delta_\xi^2\phi_{i,j} = \frac{\phi_{i+1,j} - 2\phi_{i,j} + \phi_{i-1,j}}{h^2},$$

$$\delta_\theta\phi_{i,j} = \frac{\phi_{i,j+1} - \phi_{i,j-1}}{2k}, \qquad \delta_\theta^2\phi_{i,j} = \frac{\phi_{i,j+1} - 2\phi_{i,j} + \phi_{i,j-1}}{k^2}.$$

Using (3.1a)-(3.1b) in Eq. (2.6a), we obtain

$$\delta_\xi^2\psi_{i,j}+\delta_\theta^2\psi_{i,j}-\delta_\xi\psi_{i,j}-\cot\theta\delta_\theta\psi_{i,j}-s_{i,j}-\gamma_{i,j}=0. \tag{3.2}$$

The truncation error of Eq. (3.2) is

$$\gamma_{i,j}=\left[-2\left(\frac{h^2}{12}\frac{\partial^3\psi}{\partial\xi^3}+\frac{k^2}{12}\frac{\partial^3\psi}{\partial\theta^3}\right)+\left(\frac{h^2}{12}\frac{\partial^4\psi}{\partial\xi^4}+\frac{k^2}{12}\frac{\partial^4\psi}{\partial\theta^4}\right)\right]_{i,j}+\mathcal{O}(h^4,k^4) \tag{3.3}$$

and

$$s_{i,j}=-(\sin\theta e^{3\xi}\omega)_{i,j},$$

where h and k are grid spacings ($h\neq k$) in the radial and angular directions, respectively.
   Differentiating partially the stream-function Eq. (2.6a) with respect to ξ and θ, gives

$$\frac{\partial^3\psi}{\partial\xi^3}=-\frac{\partial^3\psi}{\partial\xi\partial\theta^2}+\frac{\partial^2\psi}{\partial\xi^2}+\cot\theta\frac{\partial^2\psi}{\partial\xi\partial\theta}+\frac{\partial s}{\partial\xi}, \tag{3.4a}$$

$$\frac{\partial^4\psi}{\partial\xi^4}=-\frac{\partial^4\psi}{\partial\xi^2\partial\theta^2}-\frac{\partial^3\psi}{\partial\xi\partial\theta^2}+\cot\theta\frac{\partial^3\psi}{\partial\xi^2\partial\theta}+\frac{\partial^2\psi}{\partial\xi^2}+\cot\theta\frac{\partial^2\psi}{\partial\xi\partial\theta}+\frac{\partial^2 s}{\partial\xi^2}+\frac{\partial s}{\partial\xi}, \tag{3.4b}$$

$$\frac{\partial^3\psi}{\partial\theta^3}=-\frac{\partial^3\psi}{\partial\xi^2\partial\theta}+\frac{\partial^2\psi}{\partial\xi\partial\theta}-\csc^2\theta\frac{\partial\psi}{\partial\theta}+\cot\theta\frac{\partial^2\psi}{\partial\theta^2}+\frac{\partial s}{\partial\theta}, \tag{3.4c}$$

$$\frac{\partial^4\psi}{\partial\theta^4}=-\frac{\partial^4\psi}{\partial\xi^2\partial\theta^2}+\frac{\partial^3\psi}{\partial\xi\partial\theta^2}-\cot\theta\frac{\partial^3\psi}{\partial\xi^2\partial\theta}+\cot\theta\frac{\partial^2\psi}{\partial\xi\partial\theta}+\left(\cot^2\theta-2\csc^2\theta\right)\frac{\partial^2\psi}{\partial\theta^2}$$
$$+\csc^2\theta\cot\theta\frac{\partial\psi}{\partial\theta}+\cot\theta\frac{\partial s}{\partial\theta}+\frac{\partial^2 s}{\partial\theta^2}. \tag{3.4d}$$

Using (3.3)-(3.4d) in (3.2), we obtain

$$\left(1+\frac{h^2}{12}\right)\delta_\xi^2\psi_{i,j}+\left(1+\frac{k^2}{12}\left(\cot^2\theta+2\csc^2\theta\right)\right)\delta_\theta^2\psi_{i,j}-\delta_\xi\psi_{i,j}-\cot\theta\left(1+\frac{k^2}{4}\csc^2\theta\right)\delta_\theta\psi_{i,j}$$
$$+\left(\frac{h^2+k^2}{12}\right)\left(\delta_\xi^2\delta_\theta^2\psi_{i,j}-\cot\theta\delta_\xi^2\delta_\theta\psi_{i,j}-\delta_\xi\delta_\theta^2\psi_{i,j}+\cot\theta\delta_\xi\delta_\theta\psi_{i,j}\right)$$
$$-s_{i,j}-\frac{h^2}{12}\left(\delta_\xi^2 s_{i,j}-\delta_\xi s_{i,j}\right)-\frac{k^2}{12}\left(\delta_\theta^2 s_{i,j}-\cot\theta\delta_\theta s_{i,j}\right)=0. \tag{3.5}$$

The derivatives $\partial s/\partial\xi$, $\partial s/\partial\theta$, $\partial^2 s/\partial\xi^2$ and $\partial^2 s/\partial\theta^2$ are calculated analytically and used in Eq. (3.5) in place of difference approximations. Eq. (3.5) is the fourth order compact discretization of the governing equation (2.6a).
   By combining the non-linear terms $q_r\partial\omega/\partial\xi$, $q_\theta\partial\omega/\partial\theta$ and $-q_r\omega-q_\theta\omega\cot\theta$ on the right hand side of Eq. (2.6b) with the terms $\partial\omega/\partial\xi$, $\cot\theta\partial\omega/\partial\theta$ and $\omega\csc^2\theta$ respectively on the left hand side, we obtain

$$-\frac{\partial^2\omega}{\partial\xi^2}-\frac{\partial^2\omega}{\partial\theta^2}+c\frac{\partial\omega}{\partial\xi}+d\frac{\partial\omega}{\partial\theta}+e\omega=0, \tag{3.6}$$

where

$$c = \frac{Re}{2}e^{\xi}q_r - 1, \quad d = \frac{Re}{2}e^{\xi}q_{\theta} - \cot\theta, \quad e = \csc^2\theta - \frac{Re}{2}e^{\xi}q_r - \frac{Re}{2}e^{\xi}q_{\theta}\cot\theta.$$

Once again using (3.1a)-(3.1b) in Eq. (3.6), we obtain

$$-\delta_{\xi}^2\omega_{i,j} - \delta_{\theta}^2\omega_{i,j} + c_{i,j}\delta_{\xi}\omega_{i,j} + d_{i,j}\delta_{\theta}\omega_{i,j} + e_{i,j}\omega_{i,j} - \tau_{i,j} = 0. \tag{3.7}$$

The truncation error of Eq. (3.7) is

$$\tau_{i,j} = \left[2\left(\frac{h^2}{12}c\frac{\partial^3\omega}{\partial\xi^3} + \frac{k^2}{12}d\frac{\partial^3\omega}{\partial\theta^3}\right) - \left(\frac{h^2}{12}\frac{\partial^4\omega}{\partial\xi^4} + \frac{k^2}{12}\frac{\partial^4\omega}{\partial\theta^4}\right)\right]_{i,j} + \mathcal{O}(h^4, k^4). \tag{3.8}$$

Differentiating partially the vorticity equation (3.6) respect to ξ and θ, we obtain

$$\frac{\partial^3\omega}{\partial\xi^3} = -\frac{\partial^3\omega}{\partial\xi\partial\theta^2} + c\frac{\partial^2\omega}{\partial\xi^2} + d\frac{\partial^2\omega}{\partial\xi\partial\theta} + \left(\frac{\partial c}{\partial\xi} + e\right)\frac{\partial\omega}{\partial\xi} + \frac{\partial d}{\partial\xi}\frac{\partial\omega}{\partial\theta} + \frac{\partial e}{\partial\xi}\omega, \tag{3.9a}$$

$$\frac{\partial^4\omega}{\partial\xi^4} = -\frac{\partial^4\omega}{\partial\xi^2\partial\theta^2} - c\frac{\partial^3\omega}{\partial\xi\partial\theta^2} + d\frac{\partial^3\omega}{\partial\xi^2\partial\theta} + \left(2\frac{\partial c}{\partial\xi} + e + c^2\right)\frac{\partial^2\omega}{\partial\xi^2} + \left(2\frac{\partial d}{\partial\xi} + cd\right)\frac{\partial^2\omega}{\partial\xi\partial\theta}$$

$$+ \left(2\frac{\partial e}{\partial\xi} + \frac{\partial^2 c}{\partial\xi^2} + c\frac{\partial c}{\partial\xi} + ce\right)\frac{\partial\omega}{\partial\xi} + \left(\frac{\partial^2 d}{\partial\xi^2} + c\frac{\partial d}{\partial\xi}\right)\frac{\partial\omega}{\partial\theta} + \left(\frac{\partial^2 e}{\partial\xi^2} + c\frac{\partial e}{\partial\xi}\right)\omega, \tag{3.9b}$$

$$\frac{\partial^3\omega}{\partial\theta^3} = -\frac{\partial^3\omega}{\partial\xi^2\partial\theta} + c\frac{\partial^2\omega}{\partial\xi\partial\theta} + d\frac{\partial^2\omega}{\partial\theta^2} + \left(\frac{\partial d}{\partial\theta} + e\right)\frac{\partial\omega}{\partial\theta} + \frac{\partial c}{\partial\theta}\frac{\partial\omega}{\partial\xi} + \frac{\partial e}{\partial\theta}\omega, \tag{3.9c}$$

$$\frac{\partial^4\omega}{\partial\theta^4} = -\frac{\partial^4\omega}{\partial\xi^2\partial\theta^2} + c\frac{\partial^3\omega}{\partial\xi\partial\theta^2} - d\frac{\partial^3\omega}{\partial\xi^2\partial\theta} + \left(2\frac{\partial d}{\partial\theta} + e + d^2\right)\frac{\partial^2\omega}{\partial\theta^2} + \left(2\frac{\partial c}{\partial\theta} + cd\right)\frac{\partial^2\omega}{\partial\xi\partial\theta}$$

$$+ \left(\frac{\partial^2 c}{\partial\theta^2} + d\frac{\partial c}{\partial\theta}\right)\frac{\partial\omega}{\partial\xi} + \left(2\frac{\partial e}{\partial\theta} + \frac{\partial^2 d}{\partial\theta^2} + d\frac{\partial d}{\partial\theta} + de\right)\frac{\partial\omega}{\partial\theta} + \left(\frac{\partial^2 e}{\partial\theta^2} + d\frac{\partial e}{\partial\theta}\right)\omega. \tag{3.9d}$$

Substituting Eqs. (3.8)-(3.9d) in Eq. (3.7) gives

$$-l_{i,j}\delta_{\xi}^2\omega_{i,j} - f_{i,j}\delta_{\theta}^2\omega_{i,j} + g_{i,j}\delta_{\xi}\omega_{i,j} + o_{i,j}\delta_{\theta}\omega_{i,j} + q_{i,j}\omega_{i,j}$$

$$- \left(\frac{h^2 + k^2}{12}\right)\left(\delta_{\xi}^2\delta_{\theta}^2\omega_{i,j} - c_{i,j}\delta_{\xi}\delta_{\theta}^2\omega_{i,j} - d_{i,j}\delta_{\xi}^2\delta_{\theta}\omega_{i,j}\right) + w_{i,j}\delta_{\xi}\delta_{\theta}\omega_{i,j} = 0, \tag{3.10}$$

where the coefficients $l_{i,j}$, $f_{i,j}$, $g_{i,j}$, $o_{i,j}$, $q_{i,j}$ and $w_{i,j}$ are given by

$$l_{i,j} = 1 + \frac{h^2}{12}\left(c_{i,j}^2 - 2\delta_{\xi}c_{i,j} - e_{i,j}\right), \qquad f_{i,j} = 1 + \frac{k^2}{12}\left(d_{i,j}^2 - 2\delta_{\theta}d_{i,j} - e_{i,j}\right),$$

$$g_{i,j} = c_{i,j} + \frac{h^2}{12}\left(\delta_{\xi}^2 c_{i,j} - c_{i,j}\delta_{\xi}c_{i,j} + 2\delta_{\xi}e_{i,j} - c_{i,j}e_{i,j}\right) + \frac{k^2}{12}\left(\delta_{\theta}^2 c_{i,j} - d_{i,j}\delta_{\theta}c_{i,j}\right),$$

$$o_{i,j} = d_{i,j} + \frac{h^2}{12}\left(\delta_{\xi}^2 d_{i,j} - c_{i,j}\delta_{\xi}d_{i,j}\right) + \frac{k^2}{12}\left(\delta_{\theta}^2 d_{i,j} - d_{i,j}\delta_{\theta}d_{i,j} + 2\delta_{\theta}e_{i,j} - d_{i,j}e_{i,j}\right),$$

$$q_{i,j} = e_{i,j} + \frac{h^2}{12}\left(\delta_{\xi}^2 e_{i,j} - c_{i,j}\delta_{\xi}e_{i,j}\right) + \frac{k^2}{12}\left(\delta_{\theta}^2 e_{i,j} - d_{i,j}\delta_{\theta}e_{i,j}\right),$$

$$w_{i,j} = \frac{h^2}{6}\delta_{\xi}d_{i,j} + \frac{k^2}{6}\delta_{\theta}c_{i,j} - \left(\frac{h^2 + k^2}{12}\right)c_{i,j}d_{i,j}.$$

Eq. (3.10) is the fourth order compact discretization of Eq. (3.6). The fourth order compact differences for the coefficients c, d, and e are given by

$$c = \frac{Re}{2}\frac{e^{-\xi}}{\sin\theta}\left(\delta_\theta\psi - \frac{k^2}{6}\frac{\partial^3\psi}{\partial\theta^3}\right) - 1, \qquad d = -\frac{Re}{2}\frac{e^{-\xi}}{\sin\theta}\left(\delta_\xi\psi - \frac{h^2}{6}\frac{\partial^3\psi}{\partial\xi^3}\right) - \cot\theta,$$

$$e = \frac{Re}{2}\frac{e^{-\xi}}{\sin\theta}\left(\cot\theta\left(\delta_\xi\psi - \frac{h^2}{6}\frac{\partial^3\psi}{\partial\xi^3}\right) - \left(\delta_\theta\psi - \frac{k^2}{6}\frac{\partial^3\psi}{\partial\theta^3}\right)\right) + \csc^2\theta,$$

where $\partial^3\psi/\partial\xi^3$ and $\partial^3\psi/\partial\theta^3$ are given in Eqs. (3.4a) and (3.4c).

The two-dimensional cross derivative central difference operators on a uniform anisotropic mesh $(h \neq k)$ are given by

$$\delta_\xi\delta_\theta\phi_{i,j} = \frac{\phi_{i+1,j+1} - \phi_{i+1,j-1} - \phi_{i-1,j+1} + \phi_{i-1,j-1}}{4hk},$$

$$\delta_\xi^2\delta_\theta\phi_{i,j} = \frac{\phi_{i+1,j+1} - \phi_{i+1,j-1} + \phi_{i-1,j+1} - \phi_{i-1,j-1} - 2\phi_{i,j+1} + 2\phi_{i,j-1}}{2h^2k},$$

$$\delta_\xi\delta_\theta^2\phi_{i,j} = \frac{\phi_{i+1,j+1} - \phi_{i-1,j+1} + \phi_{i+1,j-1} - \phi_{i-1,j-1} + 2\phi_{i-1,j} - 2\phi_{i+1,j}}{2hk^2},$$

$$\delta_\xi^2\delta_\theta^2\phi_{i,j} = \frac{\phi_{i+1,j+1} + \phi_{i+1,j-1} + \phi_{i-1,j+1} + \phi_{i-1,j-1} - 2\phi_{i,j+1} - 2\phi_{i,j-1} - 2\phi_{i+1,j} - 2\phi_{i-1,j} + 4\phi_{i,j}}{h^2k^2},$$

where $\phi = $ either ψ or ω.

On the surface of the sphere, no-slip condition is applied. At far off distances $(\xi \to \infty)$ uniform flow is imposed. We now turn to the boundary condition for the vorticity, focusing our discussion on the boundary where $i = 0$. The vorticity boundary condition at $i = 0$ is derived using $\psi = \partial\psi/\partial\xi = 0$ in Eq. (2.6a). Following Briley's procedure [17] we obtain the formula

$$\omega_{0,j} = \frac{-\left(108\psi_{1,j} - 27\psi_{2,j} + 4\psi_{3,j}\right)}{18h^2\sin\theta}.$$

The algebraic system obtained from the fourth order discretized stream-vorticity equations (3.5) and (3.10) is solved using line Gauss-Seidel method. The algebraic equations for ψ and ω were solved simultaneously and the vorticity boundary condition for ω is updated after every iteration. To enhance the convergence rate, multigrid technique has been used [18] with a finest grid of 256×256. The multigrid method makes use of a hierarchy of computational grids D^k with corresponding grid functions U^k, $k = 1, 2, 3, \cdots, n$. The step size in D^k are h_k and k_k and $h_{k+1} = 0.5h_k$, $k_{k+1} = 0.5k_k$ so that as k decreases D^k becomes coarser. After 5 iterations on a fine mesh the solution switches to the next coarser grid and again after 5 iterations, it switches to the next coarser grid till it reaches the coarsest grid D^k. Let the converged solution on the grid D^k be denoted as u^k. This is prolongated to the next finer grid D^{k+1} using prolongation operator P_k^{k+1} to provide an estimate for u^{k+1} as

$$u^{k+1} = P_k^{k+1}u^k.$$

This estimate is used as an initial guess for the solution on the grid D^{k+1}. The restriction and prolongation operators which are used in this study are as follows. The restriction operator R_k^{k-1} transfers a fine grid function U^k to a coarse grid function U^{k-1}. On the other hand the prolongation operator, denoted by P_{k-1}^k, transfers a coarse grid function U^{k-1} to a fine grid function U^k. For the restriction operator, the simplest one is *injection* where by the values of a function in the coarse grid are taken to be exactly the values at the corresponding points of the next fine grid i.e.,

$$(R_k^{k-1}u^k)_{i+1,j+1} = u_{2i+1,2j+1}^k.$$

We used the above injection operator throughout the study. For the prolongation operator the simplest form is derived using linear interpolation. Prolongation by linear interpolation introduces no ambiguity when the interpolated value is desired at the mid point of the boundaries of a mesh cell. The following 9-point prolongation operator defined by Wesseling [19] is used for the present study

$$(P_{k-1}^k u^{k-1})_{2i+1,2j+1} = u_{i+1,j+1}^{k-1},$$
$$(P_{k-1}^k u^{k-1})_{2i+2,2j+1} = \frac{1}{2}\left(u_{i+1,j+1}^{k-1} + u_{i+2,j+1}^{k-1}\right),$$
$$(P_{k-1}^k u^{k-1})_{2i+1,2j+2} = \frac{1}{2}\left(u_{i+1,j+1}^{k-1} + u_{i+1,j+2}^{k-1}\right),$$
$$(P_{k-1}^k u^{k-1})_{2i+2,2j+2} = \frac{1}{4}\left(u_{i+1,j+1}^{k-1} + u_{i+1,j+2}^{k-1} + u_{i+2,j+1}^{k-1} + u_{i+2,j+2}^{k-1}\right).$$

The iterations are continued until the norm of the dynamic residuals is less than 10^{-5}. Once convergence is achieved, k is incremented by unity. This is continued until $k=n$, i.e., convergence on the desired finest grid is achieved, thus yielding the required final solution.

4   Results and discussion

To enhance the convergence rate, five different grids namely 16×16, 32×32, 64×64, 128×128 and 256×256 are chosen and the results are noted for each grid. The outer boundary is chosen as 100 times the radius of the sphere for $Re>1$ and 134.2 for $Re\leq1$. The simulations are also made with different outer domains to show the effect of the far field on the computations. The drag coefficient C_D is defined by the equation

$$C_D = \frac{D}{\pi\rho U_\infty^2 a^2},$$

where D is the total drag on the sphere, a is the radius of the sphere and ρ is the density of the fluid. The drag coefficient is composed of two parts due to the viscous and pressure

Table 1: Grid independence of fourth order accurate drag coefficient values.

Re	16×16	32×32	64×64	128×128	256×256
5	3.048	3.326	3.461	3.521	3.548
10	1.752	1.953	2.060	2.111	2.134
20	1.035	1.188	1.274	1.320	1.341
25	0.870	1.019	1.099	1.144	1.165
40	0.550	0.750	0.814	0.856	0.877
50	0.386	0.652	0.709	0.750	0.771
100	–	0.115	0.471	0.504	0.526
200	–	–	0.302	0.346	0.365

Table 2: Grid independence of far field distance.

Re	40	100	110	134.2	148.4
5	3.555	3.548	3.548	3.547	3.547
10	2.137	2.134	2.134	2.134	2.134
20	1.343	1.341	1.341	1.341	1.341
40	0.878	0.877	0.877	0.877	0.877
50	0.772	0.771	0.770	0.770	0.771
100	0.527	0.526	0.526	0.525	0.525
200	0.367	0.365	0.365	0.364	0.364

drag, respectively. The viscous drag coefficient is given by

$$C_V = -\frac{4}{Re}\int_0^\pi \omega(0,\theta)\sin^2\theta d\theta$$

and the pressure drag coefficient is

$$C_P = \frac{2}{Re}\int_0^\pi \left(\omega + \frac{\partial\omega}{\partial\xi}\right)_{\xi=0}\sin^2\theta d\theta.$$

The total drag coefficient $C_D = C_V + C_P$. The drag coefficient values obtained using different grids are tabulated in Table 1 to show the grid independence. The drag coefficient values with different outer domains are compared in Table 2.

Calculated drag coefficients for low Re from 0.1 to 1.0 are given in Table 3 along with other literature values of Goldstein [20], Proudman and Pearson [21], Chester and Breach [22], Dennis and Walker [23] and Chang and Maxey [24]. The obtained results are in agreement with all the literature values including the recent values predicted by Chang and Maxey [24]. Calculated drag coefficients for high Re from 5 to 200 are given in Table 4 along with other literature values of Leclair et al. [25], Dennis and Walker [23], Fornberg [26], Juncu and Mihail [2], Feng and Michaelides [27] and Atefi et al. [28]. Once again the results concur with all the literature values including the recent values predicted by Feng and Michaelides [27] and Atefi et al. [28]. The drag coefficients for different Reynolds numbers are compared with the experimental results of Roos and Willmarth [29] and Clift et al. [30] and analytical method by Liao [31] in Fig. 2(a) and (b). The

Table 3: Comparison of drag coefficient values with other theoretical values for low *Re*.

Re	Ref. [20]	Ref. [21]	Ref. [22]	Ref. [23]	Ref. [24]	Present results
0.1	122.23	122.05	122.09	122.10	122.60	122.52
0.2	62.22	61.94	62.01	62.02	62.20	62.09
0.3	42.20	41.87	41.95	42.02	42.10	41.95
0.4	32.19	31.82	31.91	31.91	32.00	31.88
0.5	26.17	25.78	25.88	25.85	25.90	25.82
0.6	22.16	21.76	21.88	21.85	21.90	21.77
0.7	19.29	18.90	19.03	18.96	18.90	18.87
0.8	17.13	16.76	16.91	16.76	16.80	16.70
0.9	15.46	15.10	15.28	15.10	15.10	15.00
1.0	14.11	13.78	14.00	13.72	13.70	13.66

Table 4: Comparison of drag coefficient values with other theoretical values for high *Re*.

Re	Ref. [25]	Ref. [23]	Ref. [27]	Ref. [2]	Ref. [26]	Ref. [28]	Present results
1	13.66	13.72	13.49	–	–	13.66	13.66
5	3.51	3.60	3.52	–	–	–	3.55
10	2.14	2.21	–	–	–	–	2.13
20	1.36	1.36	1.34	–	–	–	1.34
40	0.93	0.90	0.88	–	–	–	0.87
50	–	–	–	0.79	–	0.79	0.77
100	0.55	–	0.55	0.53	0.54	0.55	0.53
200	–	–	–	–	0.38	–	0.36

Table 5: Comparison of HOCS drag coefficient values with CDS-UPS and DC technique.

Re	CDS-UPS				DC technique				HOCS			
	32^2	64^2	128^2	256^2	32^2	64^2	128^2	256^2	32^2	64^2	128^2	256^2
100	NC	NC	0.403	0.473	NC	NC	0.430	0.488	0.115	0.471	0.504	0.526
200	NC	NC	NC	0.289	NC	NC	NC	0.308	NC	0.302	0.345	0.365

NC – no convergence

present results agree with the experimental data of Roos and Willmarth [29] and Clift et al. [30]. Liao [31], used Homotopy analysis method to find drag coefficients and claimed that his drag coefficient formula at the 10th order approximation agrees well with experimental results when $Re < 30$. The present results also agrees with Liao [31] in the range $Re < 30$. The drag coefficient components C_V and C_P and the total drag C_D are presented in Fig. 3 on log-log scale.

Although, 40 times radius of the sphere as far field is sufficient for $Re = 100$ and 200 (see Table 2), we simulated the flow with large domain, 110 times the radius of the sphere, to compare with the CDS-UPS scheme and DC technique. The drag coefficients at $Re = 100$ and $Re = 200$ are compared with the CDS-UPS and DC technique in Table 5. It is observed that the smallest possible grid for convergence of CDS-UPS and DC technique at $Re = 100$
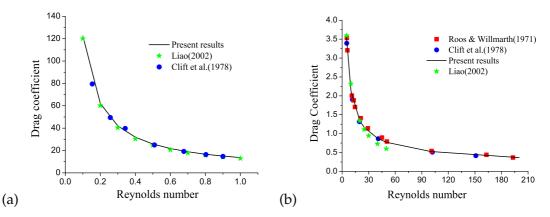
Figure 2: (a) Comparison of drag coefficient values with other experimental and theoretical values for low *Re* and (b) Comparison of drag coefficient values with experimental and theoretical values for high *Re*.
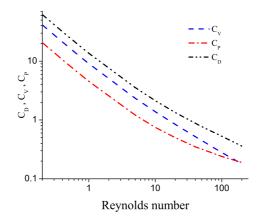

Figure 3: Distribution of drag coefficients C_V, C_P and C_D.

and $Re=200$ are 128×128 and 256×256, respectively, while for the 4th order HOCS, they are 32×32 and 64×64. It evident from Table 5 that DC technique improves the accuracy of the solution in comparison with CDS-UPS scheme and the solutions obtained by both the schemes can be achieved by the computationally inexpensive 64×64 grid by HOCS. This clearly illustrates the superiority of HOCS in comparison with CDS-UPS and DC technique and can be concluded as follows. (i) HOCS can be used in large domains (ii) HOCS gives convergence even in coarser grids (iii) Results obtained by CDS-UPS and DC technique with finer grids can be achieved by HOCS with much coarser grids.

One of the main points of interest is to determine the Reynolds number at which a separated wake first appears behind the sphere and to examine the subsequent development of the wake with Reynolds number. Various authors, including Kawaguti [32], Lister [33], Dennis and Walker [34] and Hamielec et al. [35] have found that separation has not started to occur before $Re=20$. Separated flow past a sphere has been studied experi-
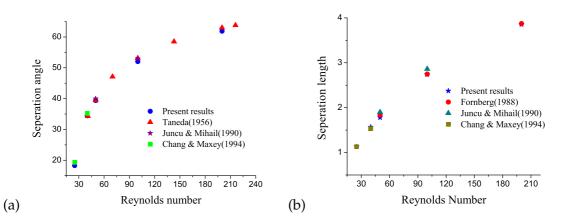
Figure 4: (a) Comparison of separation angle values with other experimental and theoretical values and (b) Comparison of separation length values with other theoretical values.
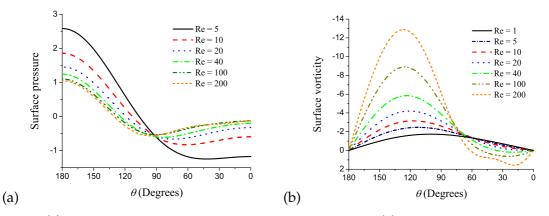

Figure 5: (a) Angular variation of the surface pressure for different Re and (b) Angular variation of the surface vorticity for same Re.

mentally by Taneda [36]. He has found that separation starts somewhere between $Re=22$ and $Re=25$ and has estimated $Re=24$ as the start of separation. Zou et al. [37], studied flow past a sphere using Domain Decomposition Method and flow separation is caught at $Re=25$. In this study, it is found that the first flow separation is occurred at $Re=21$. This prediction is slightly higher than the one predicted by Dennis and Walker [23] and Leclair et al. [25] and Pruppacher et al. [38] who estimated flow separation at 20.5, 20 and 20 respectively. Separation angles measured from the rear stagnation point for different Reynolds numbers are compared with the available data in Fig. 4(a). The present results agree with the experimental data of Taneda [36] as well as with the compared numerical results of Juncu and Mihail [2] and Chang and Maxey [24]. Separation lengths measured from the sphere center to the end of the stationary, recirculating point are compared with the available numerical results in Fig. 4(b). The present results are again in good agreement with the results of Fornberg [26] and Chang and Maxey [24].

Table 6: Comparison of surface pressure at front and rear points.

Re	Ref. [23]		Ref. [24]	Present results	
	$p(0)$	$p(\pi)$	$p(\pi)$	$p(0)$	$p(\pi)$
0.1	-60.07	62.03	62.30	-60.31	62.28
0.2	-30.05	31.97	32.10	-30.11	32.04
0.3	–	–	22.00	-20.06	21.95
0.4	–	–	16.90	-15.03	16.90
0.5	-12.02	13.86	13.90	-12.02	13.86
0.6	–	–	11.90	-10.01	11.83
0.7	–	–	10.40	-8.57	10.37
0.8	-7.52	9.29	9.29	-7.50	9.27
0.9	–	–	8.43	-6.66	8.42
1	-6.02	7.75	7.74	-5.99	7.73
5	-1.20	2.60	2.61	-1.18	2.59
10	-0.65	1.88	1.87	-0.60	1.86
20	-0.32	1.47	1.46	-0.32	1.46
40	-0.19	1.26	1.25	-0.20	1.25
50	–	–	–	-0.18	1.20
100	–	–	–	-0.15	1.10
200	–	–	–	-0.11	1.05

The surface pressure is calculated using the relations

$$p(\xi=0,\theta=\pi)=1+\frac{8}{Re}\int_0^\infty\left(\frac{\partial\omega}{\partial\theta}\right)_{\theta=\pi}d\xi$$

and

$$p(\xi=0,\theta)=1+\frac{8}{Re}\int_0^\infty\left(\frac{\partial\omega}{\partial\theta}\right)_{\theta=\pi}d\xi+\frac{4}{Re}\int_\pi^\theta\left(\omega+\frac{\partial\omega}{\partial\xi}\right)_{\xi=0}d\theta.$$

The surface pressure obtained by the above formula is presented in Fig. 5(a). The surface vorticity is also presented in Fig. 5(b). The pattern of these graphs are in good agreement with those presented by Dennis and Walker [23] and Lee [39]. The surface pressure at front and rear stagnation points of the sphere are in line with the results of Dennis and Walker [23] and Chang and Maxey [24] as shown in Table 6.

5 Conclusions

A fourth order compact scheme is developed for steady, incompressible N-S equations in spherical polar coordinates something that was not hitherto attempted. The steady, incompressible, viscous and axially symmetric flow past a sphere is used as a model problem. The HOCS is combined with multigrid method to enhance the convergence rate. The fourth order accurate solutions for the problem of viscous flow past a sphere are

presented for the first time. These values simulated over coarser grids using the present scheme are more accurate when compared to other conventional schemes. The results are in good agreement with experimental and recent theoretical results. It is found that the flow separation initially occurs at $Re = 21$. We could achieve the results with very large domain like 110 times the radius of the sphere from coarser grids using HOCS, where as CDS-UPS scheme and DC technique have failed to give the solution with coarser grids. Also, the solution obtained by the CDS-UPS and DC technique over fine grids can be achieved by computationally inexpensive coarser grids by HOCS. This shows the superiority of the HOCS in comparison with CDS-UPS and DC technique at high Reynolds numbers.

References

[1] U. Ghia, K. N. Ghia and C. T. Shin, High-Re solutions for incompressible flow using Navier-Stokes equations and a multigrid method, J. Comput. Phys., 48 (1982), 387–411.
[2] G. H Juncu and R. Mihail, Numerical solution of the steady incompressible Navier-Stokes equations for the flow past a sphere by a multigrid defect correction technique, Int. J. Numer. Meth. Fluids, 11 (1990), 379–395.
[3] T. V. S. Sekhar, R. Sivakumar, T. V. R. Ravi Kumar and K. Subbarayudu, High Reynolds number incompressible MHD flow under low R_m approximation, Int. J. Nonlinear Mech., 43 (2008), 231–240.
[4] L. Baranyi, Computation of unsteady momentum and heat transfer from a fixed circular cylinder in laminar flow, J. Comput. Appl. Mech., 4 (2003), 13–25.
[5] M. M. Gupta, High accuracy solutions of incompressible Navier-Stokes equations, J. Comput. Phys., 93 (1991), 343–359.
[6] M. Li, T. Tang and B. Fornberg, A compact fourth-order finite difference scheme for the steady incompressible Navier-Stokes equations, Int. J. Numer. Meth. Fluids, 20 (1995), 1137–1151.
[7] J. C. Kalita, D. C. Dalal and A. K. Dass, Fully compact higher order computation of steady-state natural convection in a square cavity, Phys. Rev. E, 64 (2001), 066703.
[8] W. F. Spotz and G. F. Carey, Higher order compact scheme for the steady stream-function vorticity equations, Int. J. Numer. Meth. Eng., 38 (1995), 3497–3512.
[9] E. Erturk and C. Gokcol, Fourth-order compact formulation of Navier-Stokes equations and driven cavity flow at high Reynolds numbers, Int. J. Numer. Meth. Fluids, 50 (2006), 421–436.
[10] S. R. K. Iyengar and R. P. Manohar, High order difference methods for heat equation in polar cylindrical coordinates, J. Comput. Phys., 72 (1988), 425–438.
[11] M. K. Jain, R. K. Jain and M. Krishna, A fourth-order difference scheme for quasilinear Poisson equation in polar coordinates, Commun. Numer. Methods Eng., 10 (1994), 791–797.
[12] M. C. Lai, A simple compact fourth-order Poisson solver on polar geometry, J. Comput. Phys., 182 (2002), 337–345.
[13] Y. V. S. S. Sanyasiraju and V. Manjula, Flow past an impulsively started circular cylinder using a higher-order semicompact scheme, Phys. Rev. E, 72 (2005), 016709.
[14] Y. V. S. S. Sanyasiraju and V. Manjula, Fourth-order semi compact scheme for flow past a rotating and translating cylinder, J. Sci. Comput., 30 (2007), 389–407.
[15] J. C. Kalita and R. K. Ray, A transformation-free HOC scheme for incompressible viscous flows past an impulsively started circular cylinder, J. Comput. Phys., 228 (2009), 5207–5236.

[16] R. K. Ray and J. C. Kalita, A transformation-free HOC scheme for incompressible viscous flows on nonuniform polar grids, Int. J. Numer. Fluids, 62 (2010), 683–708.

[17] W. R. Briley, A numerical study of laminar seperation bubbles using Navier-stokes equations, J. Fluid Mech., 47 (1971), 713–736.

[18] T. V. S. Sekhar, T. V. R. R. Kumar and H. Kumar, MHD flow past a sphere at low and moderate Reynolds numbers, Comput. Mech., 31 (2003), 437–444.

[19] P. Wesseling, Report NA-37, Delft University of Technology, The Netherlands, 1980.

[20] S. Goldstein, Concerning some solutions of the boundary layer equations in hydrodynamics, Proc. Cambridge Philos. Soc., 26 (1930), 1–30.

[21] I. Proudman and J. R. A. Pearson, Expansions at small Reynolds numbers for the flow past a sphere and a circular cylinder, J. Fluid Mech., 2 (1956), 237–262.

[22] W. Chester, D. R. Breach and I. Proudman, On the flow past a sphere at low Reynolds number, J. Fluid Mech., 37 (1969), 751–760.

[23] S. C. R. Dennis and J. D. A. Walker, Calculations of the steady flow past a sphere at low and moderate Reynolds numbers, J. Fluid Mech., 48 (1971), 771–789.

[24] E. J. Chang and M. R. Maxey, Unsteady flow about a sphere at low to moderate Reynolds numbers, J. Fluid Mech., 227 (1994), 347–379.

[25] B. P. Le Clair, A. E. Hamielec and H. R. Pruppracher, A numerical study of the drag on a sphere at intermediate Reynolds and Peclet numbers, J. Atmosph. Sci., 27 (1970), 308–315.

[26] B. Fornberg, Steady viscous flow past a sphere at high Reynolds numbers, J. Fluid Mech., 190 (1988), 471–489.

[27] Z. G. Feng and E. E. Michaelides, A numerical study on the transient heat transfer from a sphere at high Reynolds and Peclet numbers, Int. J. Heat Mass Trans., 43 (2000), 219–229.

[28] G. H. Atefi, H. Niazmand and M. R. Meigourpoory, Numerical analysis of 3-D flow past a stationary sphere with slip condition at low and moderate Reynolds numbers, J. Disper. Sci. Technol., 28 (2007), 591–602.

[29] F. W. Roos and W. W. Willmarth, Some experimental results on sphere and disk drag, AIAA J., 9 (1971), 285–290.

[30] R. Clift and J. R. Grace Bubbles, Drops and Particles, New York, Academic Press, 1978.

[31] S. J. Liao, An analytic approximation of the drag coefficient for the viscous flow past a sphere, Int. J. Nonlinear Mech., 37 (2002), 1–18.

[32] M. Kawaguti, Rep. Inst. Sci. Tokyo, 4 (1950), 154.

[33] M. Lister, Ph.D Thesis, London 1953.

[34] S. C. R. Dennis and M. S. Walker, Forced convection from heated spheres, Aero. Res. Counc., 26 (1964), 105.

[35] A. E. Hamielec, T. W. Hoffman and L. L. Ross, Numerical solutions of the Navier-Stokes equation for flow past spheres part I: viscous flow around spheres with finite radial mass efflux, AIChE J., 13 (1950), 212–219.

[36] S. Taneda, Experimental investigation of the wake behind a sphere at low Reynolds numbers, J. Phys. Soc. Japan, 11 (1956), 1104–1108.

[37] J.-F. Zou, A.-L. Ren and J. Deng, Numerical investigations of wake and force for flow past a sphere, Acta Aerodynamica Sinica, 03 (2004).

[38] H. R. Pruppacher, B. P. Le Clair and A. E. Hamielec, Some relations between drag and flow pattern of viscous flow past a sphere and a cylinder at low and intermediate Reynolds numbers, J. Fluid Mech., 44 (1970), 781–799.

[39] S. Lee, A numerical study of the unsteady wake behind a sphere in a uniform flow at moderate Reynolds numbers, Comput. Fluids, 29 (2000), 639–667.